LETTER • OPEN ACCESS

Chiral dichroism in bi-elliptical high-order harmonic generation

To cite this article: David Ayuso *et al* 2018 *J. Phys. B: At. Mol. Opt. Phys.* **51** 06LT01

View the article online for updates and enhancements.

You may also like

Letter

Chiral dichroism in bi-elliptical high-order harmonic generation

David Ayuso[1] , Piero Decleva[2] , Serguei Patchkovskii[1] and Olga Smirnova[1,3]

[1] Max-Born Institute for Nonlinear Optics and Short Pulse Spectroscopy, Max-Born-Straße 2A, D-12489 Berlin, Germany
[2] Dipartimento di Scienze Chimiche e Farmaceutiche, Università degli Studi di Trieste, via L. Giorgieri 1, I-34127 Trieste, Italy
[3] Technische Universität Berlin, Ernst-Ruska-Gebäude, Hardenbergstraße 36A, D-10623 Berlin, Germany

E-mail: david.ayuso-berlin.de and olga.smirnova@mbi-berlin.de

CrossMark

Abstract

The application of strong bi-elliptically polarized laser fields to the generation of high-order harmonics in organic molecules offers exceptional opportunities for chiral recognition and chiral discrimination. These fields are made by combining an elliptically polarized fundamental, typically in the infrared range, with its counter-rotating second harmonic. Here we present a theoretical study of the harmonic emission from the chiral molecule propylene oxide in bi-elliptical fields. Our calculations include, for the first time in such a complex system, accurate photorecomination matrix elements, evaluated using the static-exchange density functional theory method. We show that bi-elliptical light can induce strong chiral dichroism in the harmonic spectra of chiral molecules in a broad range of harmonic numbers and ellipticities.

An object is chiral if it cannot be superimposed on its mirror image. In chiral organic molecules, e.g. amino acids, chirality is usually a consequence of the presence of an asymmetric carbon center in their molecular structure, i.e. a carbon atom that is chemically bonded to four different constituents [1]. The investigation of enantiospecific reaction pathways [2, 3] is a key area of of modern organic chemistry because of their valuable applications, e.g. in the design of new drugs, as different enantiomers can present very different biological activity [4, 5]. Tactic polymers, which are made up of repeating units that have the same configuration [6, 7], are another important example of chiral chemistry. Polymers with different tacticity can present different physical properties and, therefore, very

different industrial and technological applications. For instance, whereas the syndiotactic version of polystyrene is a semi-crystal that presents strong resistance to heat and corrosion, its atactic version is an amorphous material [8].

Not surprisingly, finding efficient ways of detecting and quantifying chirality constitutes a topic of very active research [9–22]. The use of chiral light offers unique opportunities for chiral recognition and chiral discrimination. Today, circular dichroism absorption spectroscopy, which measures the difference in absorption between left and right circularly polarized light, is a standard method for chiral recognition [10]. Other well-established techniques are based on Raman scattering [11] or circular fluorescence [12, 13]. Several new approaches not relying on the magnetic field component of the light field have been recently demonstrated. They include microwave detection [16], Coulomb explosion imaging [17, 18] and photoelectron circular dichroism [23–27], also in the multi-photon regime [28–30]. Chiral-sensitive time-resolved techniques have seen

major advances, from the about 100 fsec resolution of vibrational circular dichroism spectroscopy [14], chiral-sensitive 2D spectroscopy [15] or time-resolved photoelectron circular dichroism [19], to photoexcitation circular dichroism [20], down to the attosecond time-resolution of chiral high-order harmonic generation spectroscopy (cHHG) [21, 22].

High-order harmonic generation (HHG) is a nonlinear process that converts intense infrared (IR) radiation into high-frequency light [31, 32]. It can be understood as a sequence of three steps: (1) tunnel ionization of an atom or a molecule induced by the strong IR field, (2) laser-driven acceleration of the electron in the continuum, and (3) recombination with the parent ion resulting in the emission of harmonic light. Since there is a well-defined relationship between the duration of the electron round-trip and the energy released upon recombination, the harmonic spectrum constitutes a series of snapshots of the laser-induced dynamics in the ion [33–41]. Interestingly, if the driving field is chiral and so is the molecular target, the process of harmonic generation can be enantiosensitive. The first implementation of cHHG exploited the chirality of elliptically polarized light for probing ultrafast chiral dynamics in propylene oxide and fenchone, with sub-femtosecond time resolution [21]. Chiral dichroism in cHHG arises from the subtle interplay between electric and magnetic effects.

One could expect that increasing the ellipticity (chirality) of the driving laser field would enhance chiral dichroism in HHG. However, as the polarization of the driving field is modified from linear to circular, the electron trajectory in the continuum deviates from a straight line and thus the electron misses recombination with the core. This difficulty can be overcome by using an elliptically polarized field in combination with its counter-rotating second harmonic, i.e. a bi-elliptical field [42–45]. Bi-elliptical fields are valuable tools for generating attosecond XUV pulses with circular and elliptical polarization [46–56], for tracking dynamical symmetry breaking [57, 58] and for bringing spin polarized electrons [59, 60] back to the ionic core [60–62]. Here we quantitatively demonstrate that such fields do indeed allow one to achieve a strong chiral response in cHHG [22]. We obtain strong chiral dichroism across the whole spectrum o f high-order harmonic emission of propylene oxide, using accurate photorecombination amplitudes and full coherent orientational averaging, thus significantly improving the pilot calculations presented in [22]. We find that chiral dichroism is achieved without relying on the interference suppression of non-chiral contributions to cHHG.

Propylene oxide is a chiral molecule because the carbon atom connected to the methyl group is an asymmetric center. Strong laser fields can induce electron tunneling from several molecular shells. In this work, we have considered four ionic states: X, A, B and C, which correlate to removing an electron from the HOMO, HOMO-1, HOMO-2 and HOMO-3 molecular orbitals of the neutral, respectively (see figure 1). As the probability of electron tunneling decreases exponentially with the ionization potential (IP), one can assume that ionization from other, deeper lying orbitals is suppressed. This results in four direct HHG channels: XX, AA, BB and CC. In this
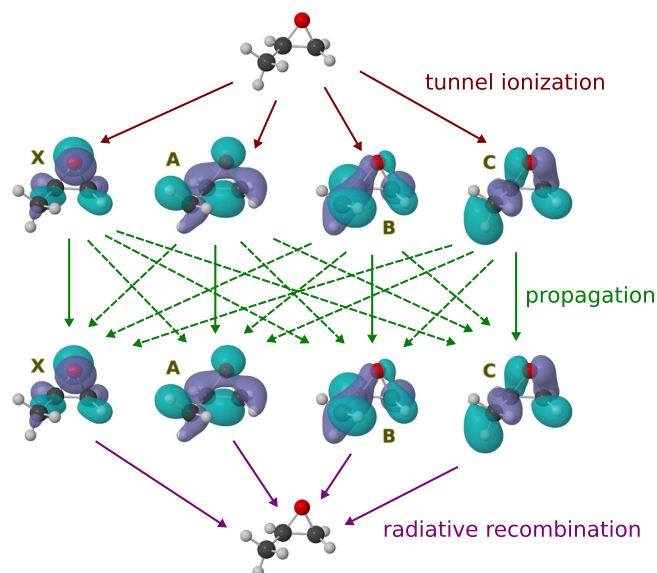

Figure 1. Schematic representation of the physical process. Strong-field ionization leaves the ion in a superposition of its electronic ground state (X) and the first three excited states (A, B and C). The molecular orbitals where the holes are created are depicted in the figure. During the electron round-trip in the continuum, the chiral laser field can induce (enantiosensitive) transitions between the ionic states, moving the hole generated upon ionization. Thus, the electron can recombine with a hole that is different from the one created upon ionization, giving rise to the emission of harmonic light that carries the signature of the multi-electron chiral dynamics.

notation, the first letter indicates the ionic state generated upon strong-field ionization and the second letter denotes the state of the ion with which the electron recombines. During the electron excursion in the continuum, the laser field can induce transitions between the different states of the core, opening up to twelve cross channels (dashed lines in figure 1). If the driving field is chiral, as in [21], these transitions can be enantiosensitive. However, their contribution to the total harmonic spectrum can be out-shined by the emission associated with the non-chiral direct channels, especially those with lower IP, which are more intense. Chiral dichroism was observed in [21] in the energy region of destructive interference between the direct channels XX and AA.

An alternative mechanism to suppress the achiral background in the harmonic spectra based on the linear Stark effect was pointed out in [22], using qualitative arguments to estimate chiral dichroism. This mechanism does not require destructive interference between different HHG channels, thus offering the possibility of measuring strong dichroism in broader regions of harmonic spectra. Our calculations confirm this expectation.

The process of high-order harmonic generation in organic molecules is extremely complex because it involves correlated multi-electron dynamics in the presence of a strong laser field. Thus, the accurate calculation of experimentally measurable quantities, such as harmonic spectra, usually requires an exhaustive computational treatment. The exact solution of the time-dependent Schrödinger equation including all degrees of freedom is out of reach, and one needs to find

J. Phys. B: At. Mol. Opt. Phys. **51** (2018) 06LT01

Letters

alternative strategies. Here we have adapted the method described in [63].

Let us consider a bi-elliptically polarized laser field created by combining two counter-rotating elliptically polarized fields with the same ellipticity ε:

$$\begin{aligned} \mathbf{F}(t) = F_0[\cos(\omega t) + \cos(2\omega t)]\hat{\mathbf{x}} \\ + \varepsilon F_0[\sin(\omega t) - \sin(2\omega t)]\hat{\mathbf{y}}, \end{aligned} \quad (1)$$

where ω is the frequency of the fundamental field. The intensity of the harmonic signal resulting from the nonlinear interaction of the laser field with the macroscopic sample of chiral molecules is given by [63]:

$$I(N\omega) \propto (N\omega)^4 |\mathbf{D}(N\omega)|^2, \quad (2)$$

where N is the harmonic number and $\mathbf{D}(N\omega)$ is the harmonic dipole in the frequency domain. For randomly oriented molecules, $\mathbf{D}(N\omega)$ results from the coherent addition of the contributions of each molecular orientation, i.e.

$$\mathbf{D}(N\omega) = \iint \mathrm{d}\Omega \int \mathrm{d}\alpha \, \mathbf{D}_{\Omega\alpha}(N\omega), \quad (3)$$

where $\mathbf{D}_{\Omega\alpha}(N\omega)$ is the harmonic dipole for a given molecular orientation. The orientation of the molecule in the laboratory frame is defined by the solid angle Ω, which accounts for all possible orientations of $\hat{\mathbf{x}}_{\mathrm{mol.}}$ (the unit vector representing the direction of the x axis of the molecular frame) and the angle α, which describes molecular rotations around the direction given by Ω. The integration over the solid angle Ω has been performed using the Lebedev quadrature [64] of order 17 and, for each value of Ω, the integration over α has been evaluated using the trapezoid method. The use of the saddle-point method [63] allows us to express $\mathbf{D}_{\Omega\alpha}(N\omega)$ as a discrete sum of ionization-recombination events:

$$\mathbf{D}_{\Omega\alpha}(N\omega) = \sum_j \sum_{mn} \mathbf{D}_{\Omega\alpha}^{jnm}(N\omega), \quad (4)$$

where j runs along the ionization bursts and the indices m and n represent the different HHG channels. Each burst contribution can be factorized into three terms:

$$\mathbf{D}_{\Omega\alpha}^{jnm}(N\omega) = a_{\mathrm{ion},\Omega\alpha}^{jnm}(N\omega) \cdot a_{\mathrm{prop},\Omega\alpha}^{jnm}(N\omega) \cdot \mathbf{a}_{\mathrm{rec},\Omega\alpha}^{jnm}(N\omega) \quad (5)$$

associated with ionization, propagation and recombination (see [63]). The main advantage of this approach is that one can evaluate these terms separately, selecting the most adequate method for each contribution, which allows one to obtain accurate results with reasonable computational resources. For the sake of simplicity, the index j and the dependence on $N\omega$ will be dropped from the following equations.

Sub-cycle ionization amplitudes are evaluated using the following expression:

$$\begin{aligned} a_{\mathrm{ion},\Omega\alpha}^{nm} = \left(\frac{2\pi}{\mathrm{i}\partial^2 S_m(t_r, t_i, \mathbf{p})/\partial t_i^2}\right)^{1/2} \\ \times \mathrm{e}^{-\mathrm{i}S_m(t_i', t_i, \mathbf{p})} \mathbf{F}(t_i') \cdot \mathbf{d}_{\mathrm{ion},m}^{\Omega\alpha}(t_i') \end{aligned} \quad (6)$$

where $t_i = t_i' + \mathrm{i}t_i''$ is the complex ionization time resulting from applying the saddle-point method [63], $\mathbf{p}$ represents

the canonical momentum, which is related to the kinetic momentum by $\mathbf{k}(t) = \mathbf{p} + \mathbf{A}(t)$, $\mathbf{A}(t)$ being the vector potential ($\mathbf{F}(t) = -\partial \mathbf{A}(t)/\partial t$), $\mathbf{d}_{\mathrm{ion},m}^{\Omega\alpha}(t_i')$ is the dipole matrix element associated with a transition from a bound orbital to the Volkov state with kinetic momentum $\mathrm{Re}\{\mathbf{k}(t_i')\}$, and S_m is given by

$$S_m(t, t', \mathbf{p}) = \frac{1}{2}\int_{t'}^t \mathrm{d}\tau[\mathbf{p} + \mathbf{A}(\tau)]^2 + \mathrm{IP}_m(t - t'). \quad (7)$$

This expression naturally provides the required sub-cycle dependence of the ionization amplitude and its connection to the sign of the ionized orbital in the direction of tunneling, but it fails to provide quantitatively accurate overall yields. For that, we use the *ab initio* results of [21] evaluated using the time-dependent resolution in ionic states method [65, 66]. That is, we renormalize $a_{\mathrm{ion},\Omega\alpha}^{nm}$ adjusting the relative ionization yields to be equal at the cutoff, in accordance with the numerical results for channels X and A [21].

Propagation amplitudes are given by

$$a_{\mathrm{prop},\Omega\alpha}^{nm} = \left(\frac{2\pi}{\mathrm{i}(t_r - t_i)}\right)^{3/2} \mathrm{e}^{-\mathrm{i}S_m(t_r', t_i', \mathbf{p})} a_{nm}^{\Omega\alpha}(t_r', t_i'), \quad (8)$$

where t_r' is the real part of the recombination time and $a_{nm}^{\Omega\alpha}$ is the transition amplitude accounting for the multi-electron dynamics induced in the ion by the laser field between ionization and recombination, which is obtained by solving the time-dependent Schrödinger equation numerically in the basis set of ionic states. The inclusion of the magnetic component of the electromagnetic field in the evaluation of $a_{nm}^{\Omega\alpha}$ is essential to describe chiral effects in HHG.

The recombination amplitude is a vector given by

$$\begin{aligned} \mathbf{a}_{\mathrm{rec},\Omega\alpha}^{nm} = \left(\frac{2\pi}{\mathrm{i}\partial^2 S_m(t_r, t_i, \mathbf{p})/\partial t_r^2}\right)^{1/2} \\ \times \mathrm{e}^{-\mathrm{i}S_m(t_r, t_r', \mathbf{p})+\mathrm{i}N\omega t_r} \mathbf{d}_{\mathrm{rec},n}^{\Omega\alpha}(\mathbf{k}_r) \end{aligned} \quad (9)$$

where $t_r = t_r' + \mathrm{i}t_r''$ is the complex recombination time and $\mathbf{d}_{\mathrm{rec},n}(\mathbf{k}_r)$ is the corresponding photorecombination matrix element, which depends on the recombination velocity $\mathbf{k}_r = \mathbf{k}(t_r)$. Photorecombination matrix elements have been evaluated using the static-exchange density functional theory (DFT) method [67, 68], which uses standard DFT to describe molecular bound states and the Galerkin approach to evaluate continuum states in the potential generated by the Kohn–Sham electron density. This method has been successfully applied to the investigation of important physical phenomena initiated by one-photon ionization in the perturbative regime, such as intramolecular photoelectron diffraction [69–74], multicenter emission [75–80], nuclear recoil [81, 82], core-hole localization [83], ultrafast charge migration [84–87] or photoelectron circular dichroism in chiral molecules [88–92]. Here we apply it, for the first time, to describe radiative electron–ion recombination in HHG.

Bound and continuum electronic states were evaluated in a multicentric basis set of B-splines and spherical harmonics. We employed a large one-center expansion (OCE) of 100 B-spline functions enclosed in a sphere of 32 a.u., with origin at the center of mass, in order to account for the long-range

J. Phys. B: At. Mol. Opt. Phys. **51** (2018) 06LT01

Letters

behavior of the continuum states, and spherical harmonics of angular momentum up to $l = 20$. The OCE was supplemented with small expansions located at the nuclear positions, which provide an accurate description of the Kato cusps [93], characteristic of the bound states. The LB94 functional [94] was employed to account for electronic exchange and correlation effects. An initial guess for the electron density was generated with the Amsterdam Density Functional computational package [95–97] using a double ζ-polarization basis set. The molecular orbitals where the holes are created in the electronic states considered in this work are depicted in figure 1.

The coherent addition of contributions from different HHG channels is very sensitive to the angular dependence of both intensities and relative phases of ionization and recombination amplitudes. While the calculation of sub-cycle ionization amplitudes in complex molecular systems is very challenging, this quantity can be reconstructed from multi-dimensional HHG measurements [39–41]. The reconstruction of the sub-cycle ionization dynamics in CO_2 molecules performed in [41] yielded virtually zero relative ionization phases in the mid-IR regime for all channels, for which reconstruction was possible in a wide range of harmonic numbers. Unfortunately, a similar reconstruction procedure is not possible in this case due to the lack of available experimental data. We note that in bi-elliptical fields the quasistatic ionization regime is approached with higher accuracy than in linear fields at the same fundamental frequency. Within the span of ionization times, the sub-cycle variations of the magnitude of the bi-elliptical field strongly decrease with the increase of ellipticity. Therefore, we expect that there is no accumulation of interchannel phases associated with non-adiabatic ionization dynamics and evaluate sub-cycle ionization amplitudes using a model that takes into account the sign of the molecular orbital from where the electron tunnels (see equation (6)). Regarding recombination, we note that the static-exchange DFT method can provide very accurate values of amplitudes and phases of transition matrix elements between bound and continuum electronic states. This is shown by the excellent agreement between the computed dichroism parameter in the one-photon ionization of propylene oxide with experimental results obtained with synchrotron radiation [88, 90].

To examine the differences in the nonlinear response of opposite enantiomers, we analyze the chiral dichroism in the harmonic intensity, defined as [10]

$$CD = 2 \frac{I_R - I_S}{I_R + I_S}, \tag{10}$$

where I_R and I_S are the harmonic intensities of R and S enantiomers, respectively. The exchange of enantiomers is equivalent to the reversal of light polarization, which can be experimentally easier to realize, especially in situations where only one enantiomer is available, and avoids additional renormalization of the experimental data due to different concentrations in the cells. We have considered two-color bi-elliptical laser fields with amplitude $F_0 = 0.034$ a.u. ($I_0 = 5 \times 10^{13}$ W cm^{-2} for linear polarization), fundamental
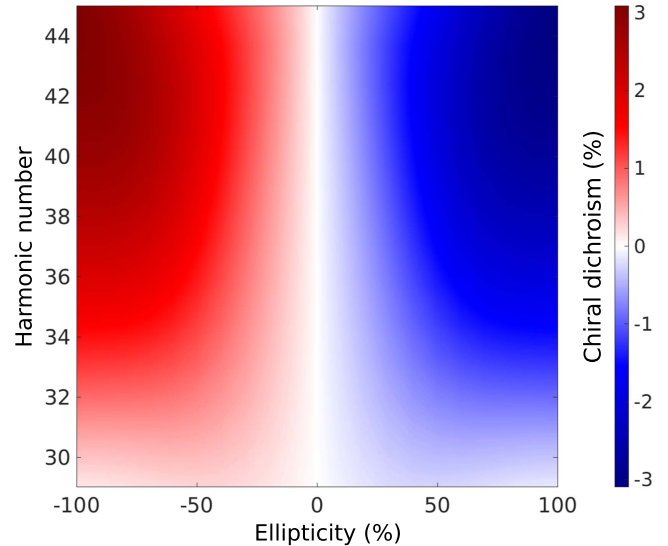

Figure 2. Chiral dichroism in high-order harmonic emission of propylene oxide as a function of ellipticity and harmonic number. Results have been calculated using the method described in the text for laser fields with electric field amplitude $F_0 = 0.034$ a.u., frequency $\omega = 0.024$ a.u. and ellipticities varying from -100% to 100%.

frequency $\omega = 0.024$ a.u. ($\lambda = 1900$ nm) and ellipticity $\varepsilon \in [-1, 1]$ (see equation (1)). The use of long laser pulses with bi-circular polarization ($\varepsilon = 1$) leads to cancellation of every third harmonic due to symmetry if the molecules are randomly oriented [57]. However, for all $\varepsilon < 1$ these harmonics are allowed and chiral dichroism (equation (10)) is well defined. Our calculations have been performed using a single ionization burst, which is a technically convenient procedure to avoid division by zero in the calculation of chiral dichroism in the regions of the spectra where high-order harmonic intensity is suppressed due to the discrete nature of the harmonic spectrum.

Chiral dichroism is shown in figure 2, as a function of ellipticity and harmonic number. For very small ellipticities, the harmonic response of R and S enantiomers is very similar (identical for $\varepsilon = 0$), and chiral dichroism is close to zero (zero for $\varepsilon = 0$). As ellipticity increases, the driving field acquires chirality and opposite enantiomers start to respond differently. In contrast to the situation in one-color fields [21], where the harmonic signal vanishes for $\varepsilon \simeq 10\%$–15%, the application of two-color fields enables the generation of harmonic light at high ellipticities, where we find a strong chiral response.

We note that the values of chiral dichroism presented in figure 2 are smaller than those previously reported in [22], obtained using a simple model based on the strong-field approximation without including accurate recombination amplitudes and full orientational averaging. As described above, the present calculations include accurate photo-recombination matrix elements and full coherent orientational averaging. Thus, it is not surprising that the simple model employed in [22] could not anticipate the values presented here. However, despite its simplicity, the model predicted strong chiral dichroism in a broad range of harmonic numbers

and ellipticities, which is confirmed by our full numerical calculations.

The results presented here confirm that, when the driving field has bi-elliptical polarization, chiral dichroism does not require destructive interference between the direct, non-chiral, channels. Indeed, large values of dichroism can be observed in a broad range of harmonic numbers. This constitutes a clear advantage with respect to the use of one-color fields, as in the first cHHG experiments [21], where chiral dichroism could only be observed in the dynamical region of destructive interference. In bi-elliptical fields, the enantiosensitive response of cross channels can be observed in a broad range of harmonic numbers because the achiral background associated with the direct channels drops with ellipticity. The mechanism responsible for this suppression is based on the linear Stark effect (see [22]), and will be discussed in detail elsewhere. Briefly, as a consequence of the interaction of the ionic states with the laser field, these accumulate a large additional phase during the electron round-trip. This extra phase depends on the relative orientation of the molecule with respect to the laser field, inducing a strong suppression of achiral background upon coherent addition of harmonic light emitted from different orientations in a sample of randomly oriented molecules. Higher-order harmonics are associated with longer excursion times, which result in stronger suppression of the achiral background, leading to stronger chiral dichroism, as shown in figure 2.

In conclusion, we have presented a procedure to describe high-order harmonic emission in complex organic molecules, and the outcome of its application to the chiral molecule propylene oxide in bi-elliptical laser fields. Our results quantify the qualitative predictions reported in [22], based on a simple model, which already anticipated strong chiral dichroism in a broad range of harmonic numbers and ellipticities. Chiral dichroism in bi-elliptical HHG takes advantage of the strong linear ε-dependent Stark shift associated with the orthogonal component of the bi-circular field, which cannot be achieved with a single-color elliptically polarized driver. As a result, destructive interference between direct HHG channels is not required, a clear advantage compared to single-color fields [21]. We have shown numerically that such a mechanism can give rise to experimentally measurable chiroptical responses in broad ranges of harmonic spectra, offering new opportunities for chiral recognition and chiral discrimination. It has been shown that subtle modifications of the parameters of the applied radiation, e.g. the relative intensities of the counter-rotating fields, can alter significantly the properties of the emitted harmonic light [55, 56]. Thus, we expect that, in the near future, similar tailoring of the driving fields can allow one to control and enhance the chiral response in cHHG.

Acknowledgments

ORCID iDs

David Ayuso ⓘ https://orcid.org/0000-0002-5394-5361
Piero Decleva ⓘ https://orcid.org/0000-0002-7322-887X
Olga Smirnova ⓘ https://orcid.org/0000-0002-7746-5733

References

[1] Wade L G 2003 *Organic Chemistry* (Englewood Cliffs, NJ: Prentice-Hall)
[2] Yoon T P and Jacobsen E N 2003 *Science* **299** 1691
[3] Mohr J T, Krout M R and Stoltz B M 2008 *Nature* **455** 323
[4] Reddy I K and Mehvar R 2004 *Chirality in Drug Design and Development* (Boca Raton, FL: CRC Press)
[5] Brooks W H, Guida W C and Daniel K G 2011 *Curr. Top. Med. Chem.* **11** 760
[6] Mark J E 2007 *Physical Properties of Polymers Handbook* (New York: Springer)
[7] Niessner N 2013 *Practical Guide to Structures, Properties and Applications of Styrenic Polymers* (Shawbury: Smithers Rapra)
[8] Ishihara N 1995 *Macromol. Symp.* **89** 553
[9] Labuta J, Ishihara S, Ikorsk T, Futera Z, Shundo A, Hanykov L, Burda J V, Ariga K and Hill J P 2013 *Nat. Commun.* **4** 2188
[10] Berova N, Polavarapu P L, Nakanishi K and Woody R W 2013 *Comprehensive Chiroptical Spectroscopy* (New York: Wiley)
[11] Parchansky V, Kapitan J and Bour P 2014 *RSC Adv.* **4** 57125
[12] Tinoco I and Turner D H 1976 *J. Am. Chem. Soc.* **98** 6453
[13] Castiglioni E, Abbate S, Lebon F and Longhi G 2014 *Methods Appl. Fluorescence* **2** 024006
[14] Rhee H, June Y-G, Lee J-S, Lee K-K, Ha J-H, Kim Z H, Jeon S-J and Cho M 2009 *Nature* **458** 310
[15] Fidler A F, Singh V P, Long P D, Dahlberg P D and Engel G S 2014 *Nat. Commun.* **5** 3286
[16] Patterson D, Schnell M and Doyle J M 2013 *Nature* **497** 475
[17] Pitzer M *et al* 2013 *Science* **341** 1096
[18] Herwig P *et al* 2013 *Science* **342** 1084
[19] Beaulieu S *et al* 2016 *Faraday Discuss.* **194** 325
[20] Beaulieu S *et al* 2018 *Nat. Phys.* (https://doi.org/10.1038/s41567-017-0038-z)
[21] Cireasa R *et al* 2015 *Nat. Phys.* **11** 654
[22] Smirnova O, Mairesse Y and Patchkovskii S 2015 *J. Phys. B: At. Mol. Opt. Phys.* **48** 234005
[23] Ritchie B 1976 *Phys. Rev.* A **13** 1411
[24] Powis I 2000 *J. Chem. Phys.* **112** 301
[25] Böwering N, Lischke T, Schmidtke B, Müller N, Khalil T and Heinzmann U 2001 *Phys. Rev. Lett.* **86** 1187
[26] Garcia G A, Nahon L, Daly S and Powis I 2013 *Nat. Commun.* **4** 2132
[27] Janssen M H M and Powis I 2014 *Phys. Chem. Chem. Phys.* **16** 856
[28] Lehmann C S, Ram N B, Powis I and Janssen M H M 2013 *J. Chem. Phys.* **139** 234307

J. Phys. B: At. Mol. Opt. Phys. **51** (2018) 06LT01

Letters

[29] Lux C, Wollenhaupt M, Bolze T, Liang Q, Khler J, Sarpe C and Baumert T 2012 *Angew. Chem., Int. Ed.* **51** 5001
[30] Lux C, Wollenhaupt M, Sarpe C and Baumert T 2015 *ChemPhysChem* **16** 115
[31] Ferray M, L'Huillier A, Li X F, Lompre L A, Mainfray G and Manus C 1988 *J. Phys. B: At. Mol. Opt. Phys.* **21** L31
[32] Corkum P B 1993 *Phys. Rev. Lett.* **71** 1994
[33] Lein M 2005 *Phys. Rev. Lett.* **94** 053004
[34] Baker S, Robinson J S, Haworth C A, Teng H, Smith R A, Chirilă C C, Lein M, Tisch J W G and Marangos J P 2006 *Science* **312** 424
[35] Baker S *et al* 2008 *Phys. Rev. Lett.* **101** 053901
[36] Smirnova O, Mairesse Y, Patchkovskii S, Dudovich N, Villeneuve D, Corkum P and Ivanov M Y 2009 *Nature* **460** 972
[37] Smirnova O, Patchkovskii S, Mairesse Y, Dudovich N and Ivanov M Y 2009 *Proc. Natl Acad. Sci.* **106** 16556
[38] Shafir D, Soifer H, Bruner B D, Dagan M, Mairesse Y, Patchkovskii S, Ivanov M Y, Smirnova O and Dudovich N 2012 *Nature* **485** 343
[39] Serbinenko V and Smirnova O 2013 *J. Phys. B: At. Mol. Opt. Phys.* **46** 171001
[40] Pedatzur O *et al* 2015 *Nat. Phys.* **11** 815
[41] Bruner B D *et al* 2016 *Faraday Discuss.* **194** 369
[42] Eichmann H, Egbert A, Nolte S, Momma C, Wellegehausen B, Becker W, Long S and McIver J K 1995 *Phys. Rev. A* **51** R3414
[43] Long S, Becker W and McIver J K 1995 *Phys. Rev. A* **52** 2262
[44] Milošević D B, Becker W and Kopold R 2000 *Phys. Rev. A* **61** 063403
[45] Milošević D B and Becker W 2000 *Phys. Rev. A* **62** 011403
[46] Zuo T and Bandrauk A D 1995 *J. Nonlinear Opt. Phys. Mater.* **04** 533
[47] Ivanov M and Pisanty E 2014 *Nat. Photon.* **8** 501
[48] Fleischer A, Kfir O, Diskin T, Sidorenko P and Cohen O 2014 *Nat. Photon.* **8** 543
[49] Pisanty E, Sukiasyan S and Ivanov M 2014 *Phys. Rev. A* **90** 043829
[50] Kfir O *et al* 2015 *Nat. Photon.* **9** 99
[51] Milošević D B 2015 *Opt. Lett.* **40** 2381
[52] Medišauskas L, Wragg J, van der Hart H and Ivanov M Y 2015 *Phys. Rev. Lett.* **115** 153001
[53] Mauger F, Bandrauk A D and Uzer T 2016 *J. Phys. B: At. Mol. Opt. Phys.* **49** 10LT01
[54] Bandrauk A D, Mauger F and Yuan K-J 2016 *J. Phys. B: At. Mol. Opt. Phys.* **49** 23LT01
[55] Dorney K M *et al* 2017 *Phys. Rev. Lett.* **119** 063201
[56] Jiménez-Galán A, Zhavoronkov N, Ayuso D, Schloz M, Morales F, Patchkovskii S, Pisanty E, Smirnova O and Ivanov M 2018 *Phys. Rev. A* **97** 023409
[57] Baykusheva D, Ahsan M S, Lin N and Wörner H J 2016 *Phys. Rev. Lett.* **116** 123001
[58] Jiménez-Galán Á, Zhavoronkov N, Schloz M, Morales F and Ivanov M 2017 *Opt. Express* **25** 22880
[59] Barth I and Smirnova O 2013 *Phys. Rev. A* **88** 013401
[60] Hartung A *et al* 2016 *Nat. Photon.* **10** 526
[61] Milošević D B 2016 *Phys. Rev. A* **93** 051402
[62] Ayuso D, Jiménez-Galán A, Morales F, Ivanov M and Smirnova O 2017 *New J. Phys.* **19** 073007
[63] Smirnova O and Ivanov M 2014 Multielectron high harmonic generation: simple man on a complex plane *Attosecond and XUV Physics* (Weinheim: Wiley) pp 201–56
[64] Lebedev V I and Laikov D N 1999 *Dokl. Math.* **59** 477
[65] Spanner M and Patchkovskii S 2009 *Phys. Rev. A* **80** 063411
[66] Spanner M, Patchkovskii S, Zhou C, Matsika S, Kotur M and Weinacht T C 2012 *Phys. Rev. A* **86** 053406
[67] Toffoli D, Stener M, Fronzoni G and Decleva P 2002 *Chem. Phys.* **276** 25
[68] Bachau H, Cormier E, Decleva P, Hansen J E and Martn F 2001 *Rep. Prog. Phys.* **64** 1815
[69] Plésiat E, Argenti L, Kukk E, Miron C, Ueda K, Decleva P and Martín F 2012 *Phys. Rev. A* **85** 023409
[70] Carroll T X, Zahl M G, Brve K J, Sthre L J, Decleva P, Ponzi A, Kas J J, Vila F D, Rehr J J and Thomas T D 2013 *J. Chem. Phys.* **138** 234310
[71] Ueda K *et al* 2013 *J. Chem. Phys.* **139** 124306
[72] Patanen M *et al* 2014 *J. Phys. B: At. Mol. Opt. Phys.* **47** 124032
[73] Ayuso D *et al* 2015 *J. Phys. Chem. A* **119** 5971
[74] Boll R *et al* 2014 *Faraday Discuss.* **171** 57
[75] Canton S E, Plsiat E, Bozek J D, Rude B S, Decleva P and Martn F 2011 *Proc. Natl Acad. Sci.* **108** 7302
[76] Plesiat E, Decleva P and Martin F 2012 *Phys. Chem. Chem. Phys.* **14** 10853
[77] Argenti L *et al* 2012 *New J. Phys.* **14** 033012
[78] Kushawaha R K, Patanen M, Guillemin R, Journel L, Miron C, Simon M, Piancastelli M N, Skates C and Decleva P 2013 *Proc. Natl Acad. Sci.* **110** 15201
[79] Patanen M *et al* 2013 *Phys. Rev. A* **87** 063420
[80] Ilchen M *et al* 2014 *Phys. Rev. Lett.* **112** 023001
[81] Kukk E *et al* 2013 *Phys. Rev. A* **88** 033412
[82] Kukk E *et al* 2017 *Phys. Rev. A* **95** 042509
[83] Guillemin R *et al* 2015 *Nat. Commun.* **6** 6166
[84] Calegari F *et al* 2014 *Science* **346** 336
[85] Calegari F *et al* 2015 *IEEE J. Sel. Top. Quantum Electron.* **21** 1
[86] Lara-Astiaso M, Ayuso D, Tavernelli I, Decleva P, Palacios A and Martin F 2016 *Faraday Discuss.* **194** 41
[87] Ayuso D, Palacios A, Decleva P and Martin F 2017 *Phys. Chem. Chem. Phys.* **19** 19767
[88] Turchini S, Zema N, Contini G, Alberti G, Alagia M, Stranges S, Fronzoni G, Stener M, Decleva P and Prosperi T 2004 *Phys. Rev. A* **70** 014502
[89] Stener M, Fronzoni G, Tommaso D D and Decleva P 2004 *J. Chem. Phys.* **120** 3284
[90] Stranges S, Turchini S, Alagia M, Alberti G, Contini G, Decleva P, Fronzoni G, Stener M, Zema N and Prosperi T 2005 *J. Chem. Phys.* **122** 244303
[91] Di Tommaso D, Stener M, Fronzoni G and Decleva P 2006 *ChemPhysChem* **7** 924
[92] Turchini S, Catone D, Contini G, Zema N, Irrera S, Stener M, Di Tommaso D, Decleva P and Prosperi T 2009 *ChemPhysChem* **10** 1839
[93] Kato T 1957 *Commun. Pure Appl. Math.* **10** 151
[94] van Leeuwen R and Baerends E J 1994 *Phys. Rev. A* **49** 2421
[95] Fonseca Guerra C, Snijders J G, te Velde G and Baerends E J 1998 *Theor. Chem. Acc.* **99** 391
[96] te Velde G, Bickelhaupt F M, Baerends E J, Fonseca Guerra C, van Gisbergen S J A, Snijders J G and Ziegler T 2001 *J. Comput. Chem.* **22** 931
[97] Baerends E J *et al* ADF2017, SCM, Theoretical Chemistry (Amsterdam: Vrije Universiteit)